Rare kaon decays from lattice QCD

Norman Christ

Physics Department, Columbia University, New York, NY 10027, USA
E-mail: nhc@phys.columbia.edu

Xu Feng[*]

Physics Department, Columbia University, New York, NY 10027, USA
E-mail: xf2131@columbia.edu

Antonin Portelli

School of Physics and Astronomy, University of Southampton, Southampton SO17 1BJ, UK
E-mail: antonin.portelli@me.com

Chris Sachrajda

School of Physics and Astronomy, University of Southampton, Southampton SO17 1BJ, UK
E-mail: cts@phys.soton.ac.uk

The rare kaon decays, $K \to \pi \ell^+ \ell^-$ and $K \to \pi \nu \bar{\nu}$, serve as ideal probes for the observation of New Physics (NP) effects. To isolate NP contributions successfully, one needs to control errors for Standard Model prediction from both short- and long-distance contributions. The RBC-UKQCD collaborations have performed a successful exploratory study on the calculation of long-distance contributions to the K_L-K_S mass difference, and are now developing necessary methods to calculate long-distance contributions to rare kaon decay amplitudes. In this proceeding, we will introduce the phenomenological background for rare kaon decays and describe the lattice methodology to calculate the corresponding decay amplitudes.

---

[*]Speaker.

1. Introduction

Rare kaon decays, described by a flavor-changing-neutral-current process, played an important role in the development of the Standard Model (SM). As a second-order electroweak interaction, SM contributions to such decay amplitudes are highly suppressed, leaving rare kaon decays ideal probes for the observation of New Physics effects.

Among various rare kaon decays, we mainly focus on two decay modes: $K \to \pi \nu \bar{\nu}$ and $K \to \pi \ell^+ \ell^-$, with a particular interest in long-distance contributions to the decay amplitudes. A proposal to calculate rare kaon decay amplitudes using lattice QCD has been made in Ref. [1]. The method to treat with a second-order electroweak amplitude on the lattice has been developed by Ref. [2] and successfully applied to the lattice calculation of K_L-K_S mass difference [3, 4]. It is recently extended to the evaluation of long-distance contributions to indirect CP violation parameter ε_K [5]. Based on these studies, we have developed the lattice method to calculate rare kaon decay amplitudes for both $K \to \pi \nu \bar{\nu}$ and $K \to \pi \ell^+ \ell^-$.

In this proceeding we briefly introduce the phenomenological background for $K \to \pi \nu \bar{\nu}$ and $K \to \pi \ell^+ \ell^-$ and describe on how to calculate corresponding decay amplitudes using lattice QCD. Some technical issues involved with our lattice methodology are also discussed.

2. Phenomenological background

2.1 $K \to \pi \ell^+ \ell^-$ decays

Due to the soft Glashow-Iliopoulos-Maiani (GIM) mechanism, CP conserving decays $K^+ \to \pi^+ \ell^+ \ell^-$ and $K_S \to \pi^0 \ell^+ \ell^-$ are long-distance dominated. Via a one-photon exchange process, amplitudes for K^+ and K_S decays can be written in terms of an electromagnetic transition form factor [6, 7]. The momentum transfer dependence of the form factor has been parameterized within the framework of chiral perturbation theory [7], where unknown parameters (or low energy constants) can be determined using the experimental data of the dilepton invariant-mass spectrum or the branching ratio as inputs. As an alternative, lattice QCD can help to provide these parameters for chiral perturbation theory. Particularly for K_S decays, the transition form factor at zero momentum transfer, a_S, is estimated to be $|a_S| = 1.06^{+0.26}_{-0.21}$ for the electron and $|a_S| = 1.54^{+0.40}_{-0.32}$ for the muon case [7]. However the sign of a_S is still unknown due to the insufficiency of the experimental data. It would be desirable if lattice QCD can determine the sign for a_S.

For CP violating K_L decays, the situation becomes more complicated. Relevant decay amplitudes receive three major contributions: 1) a short-distance dominated direct CP violation, 2) a long-distance dominated, indirect CP violating contribution through $K_L \to K_S \to \pi^0 \ell^+ \ell^-$, 3) a CP conserving component which proceeds through two-photon exchange. Total CP violating contributions to K_L decay branching ratios, including 1), 2) and their interference, are given by [8]

$$\text{Br}(K_L \to \pi^0 e^+ e^-)_{\text{CPV}} = 10^{-12} \times \left[15.7|a_S|^2 \pm 6.2|a_S| \left(\frac{\text{Im}\,\lambda_t}{10^{-4}} \right) + 2.4 \left(\frac{\text{Im}\,\lambda_t}{10^{-4}} \right)^2 \right]$$

$$\text{Br}(K_L \to \pi^0 \mu^+ \mu^-)_{\text{CPV}} = 10^{-12} \times \left[3.7|a_S|^2 \pm 1.6|a_S| \left(\frac{\text{Im}\,\lambda_t}{10^{-4}} \right) + 1.0 \left(\frac{\text{Im}\,\lambda_t}{10^{-4}} \right)^2 \right]. \quad (2.1)$$

Here $\lambda_t = V_{ts}^* V_{td}$ where $V_{qq'}$ are standard CKM matrix elements. Since a_S is a quantity of size $O(1)$ and λ_t takes the value $\text{Im}\,\lambda_t/10^{-4} \approx 1.34$, the unknown sign of a_S will cause a large uncertainty in the determination of the branching ratio. A lattice QCD study may help to clarify it.

2.2 $K \to \pi \nu \bar{\nu}$ decays

Different from $K \to \pi \ell^+ \ell^-$, the $K \to \pi \nu \bar{\nu}$ decays are known to be short-distance dominated. Long-distance contributions below the charm scale are safely neglected in $K_L \to \pi^0 \nu \bar{\nu}$ and are small in $K^+ \to \pi^+ \nu \bar{\nu}$. The SM prediction for the $K^+ \to \pi^+ \nu \bar{\nu}$ branching ratio is given by [9]

$$\text{Br}(K^+ \to \pi^+ \nu \bar{\nu}) = \left(7.81^{+0.80}_{-0.71}\text{para} \pm 0.29\text{theory} \right) \times 10^{-11}, \tag{2.2}$$

with a 10% parametric uncertainty from SM inputs (V_{cb}: 56%, $\bar{\rho}$: 21%, others 23%) and a 4% theoretical error with uncertainty coming from the long-distance contributions ($\delta P_{c,u}$: 46%), higher-order QCD and electroweak effects in the top quark contribution (X_t: 27%) and charm quark contribution (P_c: 20%), and others (7%).

To make a precise SM prediction, the top priority is to have accurate CKM matrix elements such as V_{cb} and $\bar{\rho}$. On the other hand, the long-distance contributions $\delta P_{c,u}$ are now the dominant source of the 4% theoretical uncertainty. With the inclusion of $\delta P_{c,u} = 0.04 \pm 0.02$ from chiral perturbation theory, the relevant branching ratio is enhanced by 6% [10]. Since only part of the $O(p^4)$ contributions are estimated, Ref. [10] took the $O(p^2)$ result as the central value and attributed to it a 50% error. Although the error is assigned conservatively, the ignorance of the relevant $O(p^4)$ contributions opens the possibility that the long-distance contributions may be larger than expected. A lattice calculation of long-distance contributions from first principles can help to reduce this uncertainty.

Considering the fact that NA62 in CERN [11] plans to obtain $O(100)$ total $K^+ \to \pi^+ \nu \bar{\nu}$ events in two years and make a 10%-precision measurement of the branching ratio, an accurate determination of the long-distance contribution to the $K^+ \to \pi^+ \nu \bar{\nu}$ branching ratio is of importance.

3. Lattice setup

At the quark level, these rare kaon decay amplitudes can be induced by γ/Z-exchange and box diagrams, containing up, charm and top quarks. For $K \to \pi \ell^+ \ell^-$ decays, γ-exchange diagrams dominate the amplitude; for $K \to \pi \nu \bar{\nu}$, we need to evaluate the long-distance contributions to both Z-exchange and the W-box diagrams.

3.1 γ/Z-exchange diagrams

In Minkowski space the non-local hadronic matrix element in γ/Z-exchange diagrams can be written in terms of the form factor $F_i^{\gamma,Z}(q^2)$ through [7]

$$
\begin{aligned}
T_\mu^{\gamma,Z}(q^2) &= i \int d^4x \, \langle \pi(p_\pi)| T\{J_\mu^{\gamma,Z}(0) H_W(x)\} |K(p_K)\rangle \\
&= F_1^{\gamma,Z}(q^2) q^2 (p_K + p_\pi)_\mu - F_2^{\gamma,Z}(q^2)(m_K^2 - m_\pi^2) q_\mu,
\end{aligned}
\tag{3.1}
$$

3

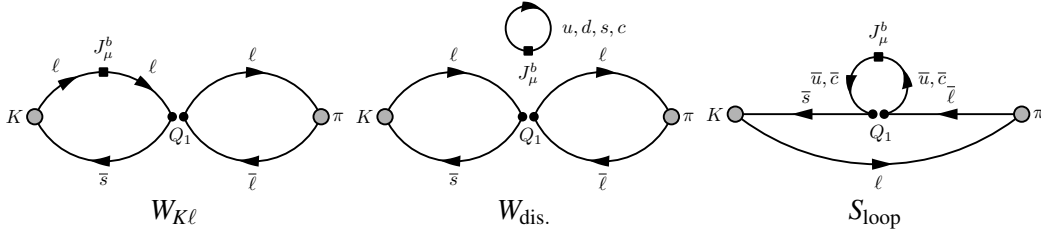**Figure 1:** Samples of contractions contributing to γ/Z-exchange diagrams. There are totally 22 types of diagrams. Here we just select three: $W_{K\ell}$ for connected, $W_{\text{dis.}}$ for disconnected and S_{loop} for loop diagrams.

where $q = p_K - p_\pi$. Here $J_\mu^{\gamma,Z}$ are the electromagnetic and neutral weak currents associated with the photon and Z-boson. The $|\Delta S| = 1$ effective Hamiltonian $H_W(x)$ is given by [1]

$$H_W = \frac{G_F}{\sqrt{2}} V_{us}^* V_{ud} \sum_{i=1,2} C_i (Q_i^u - Q_i^c),$$

$$Q_1^q = \bar{s}_\alpha \gamma^\mu (1-\gamma_5) q_\beta \, \bar{q}_\beta \gamma_\mu (1-\gamma_5) d_\alpha, \quad Q_2^q = \bar{s}_\alpha \gamma^\mu (1-\gamma_5) q_\alpha \, \bar{q}_\beta \gamma_\mu (1-\gamma_5) d_\beta, \quad (3.2)$$

with C_i the corresponding Wilson coefficients. For γ-exchange diagrams, the Ward-Takahashi identity guarantees $F_1^\gamma(q^2) = F_2^\gamma(q^2)$. Note that the $F_2^{\gamma,Z}$ term does not contribute to the amplitude. Therefore one can simply write decay amplitudes (up and charm quark contributions only) as [7]

$$A(K \to \pi \ell^+ \ell^-)_\gamma = -e^2 F_1^\gamma(q^2)(p_K + p_\pi)^\mu \bar{u}_\ell \gamma_\mu v_\ell,$$

$$A(K \to \pi \nu \bar{\nu})_Z = \frac{G_F}{2\sqrt{2}} F_1^Z(q^2) q^2 (p_K + p_\pi)^\mu \bar{u}_\nu \gamma_\mu (1-\gamma_5) v_\nu. \quad (3.3)$$

Depending on the integration range, $T_\mu^{\gamma,Z}(q^2)$ can be naturally split into two parts [12]

$$T_\mu^{\gamma,Z}(q^2) = \sum_{n_s} \frac{\langle \pi(p_\pi)|H_W(0)|n_s\rangle \langle n_s|J_\mu^{\gamma,Z}(0)|K(p_K)\rangle}{E_{n_s} - E_\pi + i\varepsilon} - \sum_n \frac{\langle \pi(p_\pi)|J_\mu^{\gamma,Z}|n\rangle \langle n|H_W|K(p_K)\rangle}{E_K - E_n + i\varepsilon}, \quad (3.4)$$

where $\{|n\rangle\}$ and $\{|n_s\rangle\}$ stand for complete sets of non-strange and strange states.

In a lattice calculation a similar expression can be obtained by evaluating the 4-point correlation function

$$\int_{-T_a}^{T_b} dt \, \langle \phi_\pi(\vec{p}_\pi, t_\pi) T[J_\mu^{\gamma,Z}(0)H_W(t)]\phi_K^\dagger(\vec{p}_K, t_K)\rangle \equiv \sqrt{Z_K}\frac{e^{-E_K|t_K|}}{2E_K} T_E^{\gamma,Z} \sqrt{Z_\pi}\frac{e^{-E_\pi t_\pi}}{2E_\pi} \quad (3.5)$$

with ϕ_π and ϕ_K interpolating operators for the pion and kaon and

$$T_E^{\gamma,Z} = \sum_{n_s} \frac{\langle \pi(p_\pi)|H_W(0)|n_s\rangle \langle n_s|J_\mu^{\gamma,Z}(0)|K(p_K)\rangle}{E_{n_s} - E_\pi} \left(1 - e^{(E_\pi - E_{n_s})T_b}\right)$$

$$- \sum_n \frac{\langle \pi(p_\pi)|J_\mu^{\gamma,Z}(0)|n\rangle \langle n|H_W(0)|K(p_K)\rangle}{E_K - E_n} \left(1 - e^{(E_K - E_n)T_a}\right) \quad (3.6)$$

Samples of diagrams for the 4-point correlation function are given in Fig. 1. Note that the second term in Eq. (3.6) suffers from exponential growing contamination at large T_a if $E_n < E_K$. For the γ-exchange diagrams, we need to remove contamination from $|n\rangle = |\pi\rangle, |3\pi\rangle$. For Z-exchange

diagrams including both vector and axial vector currents, additional contamination from $|n\rangle = |2\pi\rangle$ must be removed. (Here, $|n\rangle = |0\rangle$ does not contribute since we are only intested in K^+ decays.) This is a generic feature of non-local matrix elements in the second-order weak interaction. A similar situation happens with the K_L-K_S mass difference [3, 4].

3.2 *W*-box diagrams

In $K^+ \to \pi^+ \nu\bar\nu$ decays, in addition to the Z-exchange diagrams, we also need to evaluate the W-box diagrams. The starting point is a non-local matrix element [10]

$$T^{W,\ell} = i \int d^4x \langle \pi\nu\bar\nu | T\{O^{\Delta S=1}(x)O^{\Delta S=0}(0)\} | K\rangle_{u-c} \tag{3.7}$$

where $u - c$ indicates the GIM cancellation. The operators $O^{\Delta S=1}$ and $O^{\Delta S=0}$ are induced by replacing each W-boson exchange by an effective four-fermion operator

$$O^{\Delta S=1} = \bar{s}\gamma^\mu(1-\gamma_5)q\,\bar\nu\gamma_\mu(1-\gamma_5)\ell, \quad O^{\Delta S=0} = \bar\ell\gamma^\mu(1-\gamma_5)\nu\,\bar{q}\gamma_\mu(1-\gamma_5)d, \tag{3.8}$$

with $q = u, c$ and $\ell = e, \mu, \tau$.

Separating the hadronic and leptonic parts in $T^{W,\ell}$, we have

$$T^{W,\ell} = i \int d^4x \overbrace{\langle \pi(p_\pi) | T\{\bar{s}\gamma_\alpha(1-\gamma_5)q(x)\,\bar{q}\gamma_\beta(1-\gamma_5)d(0)\} | K(p_K)\rangle}^{H_{\alpha\beta}(x):\text{ hadronic part}}$$
$$\times \underbrace{\bar{\mathrm{u}}(p_\nu)\gamma^\alpha(1-\gamma_5)S_\ell(x,0)\gamma^\beta(1-\gamma_5)\mathrm{v}(p_{\bar\nu})e^{-ip_\nu x}}_{\bar{\mathrm{u}}(p_\nu)\Gamma^{\alpha\beta}(x)\mathrm{v}(p_{\bar\nu}):\text{ leptonic part}}. \tag{3.9}$$

where $\mathrm{u}(p_\nu)$ and $\mathrm{v}(p_{\bar\nu})$ are Dirac plane-wave spinors and $S_\ell(x,0)$ the lepton propagator. Because of the chiral property of the spinors $\bar{u}(p_\nu)$ and $v(p_{\bar\nu})$, the can only enter the final result is the combination $T^{W,\ell} = T^\mu \bar{\mathrm{u}}(p_\nu)\gamma_\mu(1-\gamma_5)\mathrm{v}(p_{\bar\nu})$. Assuming massless neutrinos, the Lorentz structure of T^μ can be further simplified as $T^\mu = F^\ell(p_K, p_\nu, p_{\bar\nu})p_K^\mu$. Thus, we have

$$T^{W,\ell} = i \int d^4x H_{\alpha\beta}(x)\bar{\mathrm{u}}(p_\nu)\Gamma^{\alpha\beta}(x)\mathrm{v}(p_{\bar\nu}) = F^\ell(p_K, p_\nu, p_{\bar\nu})\bar{\mathrm{u}}(p_\nu)\slashed{p}_K(1-\gamma_5)\mathrm{v}(p_{\bar\nu}). \tag{3.10}$$

It can be shown that the form factor $F^\ell(p_K, p_\nu, p_{\bar\nu})$ can be obtained through

$$F^\ell(p_K, p_\nu, p_{\bar\nu}) = \frac{i\int d^4x H_{\alpha\beta}(x)\,\mathrm{Tr}[\Gamma^{\alpha\beta}(x)\slashed{p}_{\bar\nu}\slashed{p}_K(1-\gamma_5)\slashed{p}_\nu]}{\mathrm{Tr}[\slashed{p}_K(1-\gamma_5)\slashed{p}_{\bar\nu}\slashed{p}_K(1-\gamma_5)\slashed{p}_\nu]}. \tag{3.11}$$

Using $F^\ell(p_K, p_\nu, p_{\bar\nu})$ the decay amplitude for the W-box diagrams can be written as

$$A(K \to \pi\nu\bar\nu)_W = G_F^2 V_{us}^* V_{ud} \sum_{\ell=e,\mu,\tau} F^\ell(p_K, p_\nu, p_{\bar\nu})p_K^\mu \bar{\mathrm{u}}(p_\nu)\gamma_\mu(1-\gamma_5)\mathrm{v}(p_{\bar\nu}). \tag{3.12}$$

In a lattice calculation, the hadronic matrix element $H_{\alpha\beta}$ can be calculated by constructing a 4-point correlation function. The leptonic propagator can be implemented using a lattice fermion formulation, such as domain wall or overlap fermion. Following the steps described above one can determine the decay amplitude. The quark and lepton contractions for $T^{W,\ell}$ are given in Fig. 2. In the type 1 diagram, the intermediate state is given by a single lepton state $|\ell\rangle$ or hadronic states carrying no flavor quantum numbers such as $|\ell, 2\pi\rangle$. The type 2 diagram is mediated by the states of $|\ell, \pi\rangle, |\ell, 3\pi\rangle, \cdots$. As in the case of the γ/Z-exchange diagrams, if an intermediate state energy is lower than the initial kaon energy, then exponential growing contamination needs to be removed.
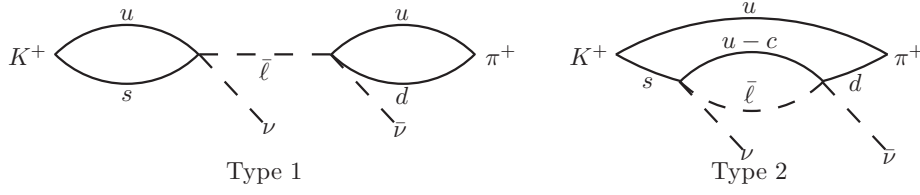
Figure 2: Quark and lepton contractions for W-box diagrams.

4. Technical issues

4.1 Short-distance divergences on the lattice

In the calculation of γ/Z-exchange diagrams, when the $J_\mu^{\gamma,Z}$ operator approaches to the H_W operator in the S_{loop} diagram in Fig. 1, a potential quadratic divergence is allowed by dimensional counting. Ref. [1] pointed out that in γ-exchange diagrams, if a conserved vector current is used, then an external momentum factor $q^2\delta_{\mu\nu} - q_\mu q_\nu$ can be extracted and correspondingly, the diagram is reduced to be logarithmic divergent. Further GIM mechanism cancels this logarithmic divergence. Thus no lattice to continuum matching is required.

The situation is different for Z-exchange diagrams. The non-zero quark mass m_q, $q = u,c$ breaks the chiral symmetry explicitly. There exists another allowed tensor structure $m_q^2\delta_{\mu\nu}$, which reduces the degree of divergence by 2 but now the GIM mechanism cannot cancel the logarithmic divergence. So if either a conserved or local axial vector current is used, after GIM cancellation, we need to deal with a similar logarithmic divergence.

A similar situation happens with the W-box diagrams, which appear to be quadratically divergent by dimensional counting. The V-A structure of the weak current and GIM mechanism reduce the divergence to logarithmic. (This is different from the K_L-K_S mass difference where the double GIM cancellation makes W-box diagrams ultraviolet finite [3].)

In both Z-exchange and W-box diagrams, the short-distance divergence is cut off by the lattice spacing, rather than the physical Z or W mass. This can be corrected by removing the short-distance part of the lattice result and adding back the correct, continuum short-distance contribution through

$$A - A_{SD}^{lat} + A_{SD}^{cont} = \int d^4x \langle \pi | T\{O_1(x)O_2(0)\}|K\rangle - \langle \pi | C^{lat}(\mu^2)O_{SD}|K\rangle + \langle \pi | C^{cont}(\mu^2)O_{SD}|K\rangle \quad (4.1)$$

where $O_{1,2}$ stands for J_μ^Z, H_W (Z-exchange) and $O^{\Delta S=1}$, $O^{\Delta S=0}$ (W-box). The short-distance operator O_{SD} is given by $\bar{s}\gamma^\mu(1-\gamma_5)d\,\bar{\nu}\gamma_\mu(1-\gamma_5)\nu$. The Wilson coefficient $C^{lat}(\mu^2)$ on the lattice can be determined using the non-perturbative Rome-Southampton RI/MOM approach [13], while $C^{cont}(\mu^2)$ in the continuum can be calculated perturbatively.

4.2 Finite-volume effects

Concerning the second-order weak amplitude where the intermediate state involves multiple particles, Refs. [2, 14] have given the detailed formulae to evaluate the finite-volume (FV) correction to the K_L-K_S mass difference. The same approach can be used to determine FV effects in rare kaon decay amplitudes.

Important information from the FV study is that the power-like, FV correction is related to the square of the on-shell amplitude $A(K \to \{n\})$, where $\{n\}$ stands for n particles in the intermediate

states. If the number of particles increases, we expect that the FV correction is suppressed by a phase-space factor. The decay rate $\Gamma(K_L \to 3\pi)/\Gamma(K_S \to 2\pi) = 5.6 \times 10^{-3}$ suggests that the FV correction induced by the on-shell 3π-state may be ~ 100 times smaller than that from the 2π-state.

Thus, we focus on the 2-particle state. In γ-exchange diagrams, we consider a matrix element $\langle \pi(p_\pi)|J_\mu^\gamma|\pi(p_1)\pi(p_2)\rangle$, which carries the possible Lorentz factor $p_{\pi,\mu}$, $p_{1,\mu}$, $p_{2,\mu}$ and $\varepsilon_{\mu\nu\rho\sigma}p_\pi^\nu p_1^\rho p_2^\sigma$. The $\varepsilon_{\mu\nu\rho\sigma}$ term does not contribute to the decay amplitude because after the momentum integral, there are only two independent momenta in p_π and $q = p_K - p_\pi$ and an $\varepsilon_{\mu\nu\rho\sigma}$ structure cannot be constructed. The terms proportional to $p_{\pi,\mu}$, $p_{1,\mu}$ and $p_{2,\mu}$ vanish as well due to parity symmetry. In Z-exchange diagrams, since the axial vector current is involved, the 2π-state contributes to the decay amplitude. In the W-box diagrams, a 2-particle state $|\ell, \pi\rangle$ appears in the type 2 diagram in Fig. 2. For these cases FV corrections must be estimated properly.

5. Conclusion

With the development of the method [2], it is now possible to calculate long-distance contributions to the second-order weak amplitude directly using lattice QCD. Rare kaon decays are such an example [1, 12]. So far we have discussed the phenomenological background for $K \to \pi\ell^+\ell^-$ and $K \to \pi\nu\bar{\nu}$ and introduced the lattice methodology to calculate corresponding decay amplitudes. For more detailed methods and numerical results, we refer interested readers to our forthcoming papers.

References

[1] G. Isidori, G. Martinelli, and P. Turchetti, Phys.Lett. **B633**, 75 (2006), hep-lat/0506026.

[2] RBC Collaboration, UKQCD Collaboration, N. H. Christ, (2010), 1012.6034.

[3] RBC and UKQCD Collaborations, N. Christ, T. Izubuchi, C. Sachrajda, A. Soni, and J. Yu, Phys.Rev. **D88**, 014508 (2013), 1212.5931.

[4] Z. Bai *et al.*, Phys.Rev.Lett. **113**, 112003 (2014), 1406.0916.

[5] N. H. Christ, PoS **LATTICE2011**, 277 (2011), 1201.2065.

[6] G. Ecker, A. Pich, and E. de Rafael, Nucl.Phys. **B291**, 692 (1987).

[7] G. D'Ambrosio, G. Ecker, G. Isidori, and J. Portoles, JHEP **9808**, 004 (1998), hep-ph/9808289.

[8] V. Cirigliano, G. Ecker, H. Neufeld, A. Pich, and J. Portoles, Rev.Mod.Phys. **84**, 399 (2012), 1107.6001.

[9] J. Brod, M. Gorbahn, and E. Stamou, Phys.Rev. **D83**, 034030 (2011), 1009.0947.

[10] G. Isidori, F. Mescia, and C. Smith, Nucl.Phys. **B718**, 319 (2005), hep-ph/0503107.

[11] NA62 Collaboration, M. Moulson, (2013), 1310.7816.

[12] RBC-UKQCD, C. T. Sachrajda, PoS **KAON13**, 019 (2013).

[13] G. Martinelli, C. Pittori, C. T. Sachrajda, M. Testa, and A. Vladikas, Nucl.Phys. **B445**, 81 (1995).

[14] N. Christ, G. Martinelli, and C. Sachrajda, PoS **LATTICE2013**, 399 (2014), 1401.1362.